MOLECULAR DYNAMICS SIMULATION OF PHONON SCATTERING AT ROUGH SEMICONDUCTOR INTERFACES

Lin Sun, Jayathi Y Murthy
School of Mechanical Engineering
Purdue University
585 Purdue Mall,
West Lafayette, IN, USA. 47906
Phone: (765) 494-6849
Email: sun33@purdue.edu

ABSTRACT

Detailed phonon transport at a rough semiconductor interface is studied by the molecular dynamics method. The simulation results show that phonon transmission coefficient is a strong function of frequency, roughness characteristic length and atomic structure. When the roughness characteristic length is comparable to the phonon wave length, the phonon transmission is decreased significantly. Complex phonon mode conversions and wave interference effects are observed.

KEY WORDS: interface, phonon, transmission, molecular dynamics.

INTRODUCTION

As heat flows across the interface between two different materials, a temperature drop is found at the interface which may be represented by a thermal resistance. This is called thermal boundary resistance (TBR). Interface transport has been a particularly poorly understood but critically important thermal problem in recent years. Since surface-to-volume ratios increase as domain length scales fall, interface physics begin to dominate at sub-micron scales. Phonon transport across Si/SiO2 interfaces controls self-heating in emerging silicon-on-insulator (SOI) field effect transistors (FETs) [1], for example. Here the channel region of the transistor is fabricated on top of a silicon dioxide insulator. Heat generated due to electron-phonon scattering in the channel must be transported through the oxide into the bulk silicon and thence to the heat sink. The transmissivity of the Si/SiO2 interface is critical in determining the effective resistance to heat transfer in the device layer, and consequently, how hot the transistor gets. Similarly, emerging carbon nanotube (CNT) FETS[2] fabricated in SiO2 also requires a good understanding of the thermal transport of the CNT-SiO2 interface. In some applications, such as carbon nanotubes and silicon nanowires thin-film composites [3], thermal resistance at wire/substrate interfaces may limit the thermal conductivity of the composite. Similar issues arise in the fabrication of thermal interface materials for heat spreading in microelectronics [4].

However, TBR is not a newly discovered phenomenon. As early as in 1940's, Kapitza found this effect in studies of heat conduction between a solid surface and liquid helium [5]. Consequently, TBR is also referred to as Kapitza conductance. Khalatnikov [6] developed the first theoretical model to explain this phenomenon, known as the acoustic mismatch (AM) model. In this model, phonons behave like plane waves so that the transmission and reflection coefficients can be calculated from plane–wave dynamics. Moreover, the interface is assumed perfect and no scattering takes place. The thermal impedance is caused by the difference of mass density and speed of sound on the two sides of the interface, and is analogous to the propagation of light across the interface between two optically different materials. These assumptions are generally true when the temperature is extremely low and the interface is perfect. In 1987, Swartz and Pohl [7] proposed the Diffuse Mismatch (DM) model to account for phonon diffusion at the interface. This model assumes that the incident phonons encounter elastic diffuse scattering at the interface and emit to both sides. The probability of being scattered to either side of the interface is proportional the phonon density of states of that region. Furthermore, the elastic scattering assumption does not allow phonon frequency change, i.e. phonons cannot convert from mode to mode. Generally this assumption is not true. For instance, if two materials A and B have a large mismatch in their phonon dispersion relations, a certain range of phonons cannot be transmitted across the interface unless some mode conversion occurs at the interface. Thus, some inelastic scattering must happen to change the phonon frequency. This phenomenon has been proven by molecular dynamics (MD) simulation [8].

Neither the AM nor the DM model addresses the interface sturcture itself. Both theories neglect the fact that the interface atomic structure and roughness can greatly modify phonon behavior. For example, disorder and defects at the atomic level, which always exist at the interface during synthesis, can greatly scatter phonons and complicate the transport mechanism. Recently, with the growth in interest in solid-solid interfaces in nanoscale applications, there have been a series of efforts on the modeling of TBR at high temperatures by modifying the AM and DM models [9]. Experiments indicate that the DM model is not sufficient to describe heat transport at interfaces at room temperature [10].

More recently, a lattice dynamics method has been used to compute the phonon transport at the interface between two semi-infinite fcc lattices [11] and has been extended to the study of phonon scattering at ideal Si-Ge interfaces [12].

Using this technique, the frequency-dependent reflection and transmission coefficients were obtained. However, it is difficult to implement this method in the complex atomic interface structures. An alternative approach using atomistic Green's functions has been proposed to characterize the interface phonon transport [13,14]. This approach is based on a dynamical equation and the quantum mechanical description of the phonon energy distribution. Thus it is suitable for the study cases at low temperatures when phonons are ballistic. The benefit of this approach is that only equilibrium locations of atoms and the interatomic potential are needed as inputs, and phonon dispersion curves and density of states are not required. Furthermore, it is capable of dealing with complex atomic configurations. This approach has been applied to the study of phonon transport in nanowires coated with an amorphous material [**Error! Bookmark not defined.**3], and extended to handle Si-Ge heterostructures [14].

Despite all these efforts, no generally accepted theory has emerged to predict how the interface condition affects phonon transmission and it is very difficult to perform experiments to validate the proposed models. Molecular dynamics simulation provides an attractive way to help explain experimental data and in understanding the details of scattering mechanisms at the interface. In addition to its intrinsic benefits, MD is able to build well-controlled interfaces at the atomic level. Dislocations, defects, stressed boundaries and the like, which are difficult to control in experiments, can be mimicked easily. The Lennard-Jones potential has been used for MD simulation in FCC crystals due to its simplicity. Two different virtual materials may be created by adjusting mass, lattice or potential parameters, and thus form an layered interface structure between them [15-17]. Some materials with a more complicated structure and potential such as silicon grain boundaries have also been investigated [18,19]. To gain insight into the heat transfer in detail, Schelling and co-workers used the wave-packet method, described below, to calculate the transmission coefficients for different phonon modes [20]. Twu and Ho investigated the impact of interface disorder on TBR [21]. Although these simulations are still limited to simple interfaces, they have shown that MD has enormous potential in helping to understand the fundamental mechanisms of phonon interaction with interfaces.

In this paper, we apply molecular dynamics simulation and the wave-packet method to study the detailed phonon transport at a rough semiconductor interface. Two diamond-structured materials that differ only in their masses are chosen. The interface between these two semiconductors is manipulated to create a thin layer of roughness by staggering the two types of atoms at the interface. The roughness is characterized by the interval space between these two different types of atoms on the interface plane and also the thickness of the interface layer. A phonon wave packet is initialized with a pre-defined frequency and polarization and allowed to propagate through the interface. The interaction of the phonon wave packet with the interface is monitored by analyzing the simulation data in phonon wave space. The phonon transmission coefficient is calculated by measuring the phonon energy change before and after interface scattering.

SYSTEM SETUP AND SIMULATION PARAMETERS

The MD simulation domain is shown in Fig. 1(a). Two artificial materials A and B share a common interface. The initial configuration of atoms employs the lattice structure of silicon. A and B only differs in atomic mass. In particular, material A takes all the properties of silicon, i.e. $m_A = m_{Si}$, and material B is a hypothetical material with $m_B = 4m_{Si}$. When phonons travel from one material to another, transmission and reflection occur at the interface because of the different acoustic properties of A and B. Lattice mismatch also affects transmissivity and reflectivity. However, in many cases, such as for the Si/Ge interface, the influence of lattice mismatch on phonon transmission is far less than that caused by mass difference. Therefore, in this paper, we only consider the mass difference between two materials and assume that the lattice structure remains the same.

A thin layer of roughness is inserted between material A and B, and its atomic structure and thickness are manipulated as needed. Figure 1(b) shows the typical roughness structure used; here materials A and B are mixed in a regular pattern, with the interval distance being varied. Classical molecular dynamics is used to compute the evolution of a N-atom system with time using Newton's second law. A empirical potential for silicon called Environment Dependent Interatomic Potential (EDIP)[22] is used. A micro-canonical ensemble (NVE) is employed for the simulations. The boundaries in all three directions are assumed periodic so that the atoms leaving a bounding surface re-enter the domain through the corresponding periodic face on the opposite side. A time step $\Delta t = 1$ fs is used. The entire simulation domain involves up to 1 million atoms. In order to the keep the simulation time tractable, parallel processing using a domain decomposition paradigm is used [23].

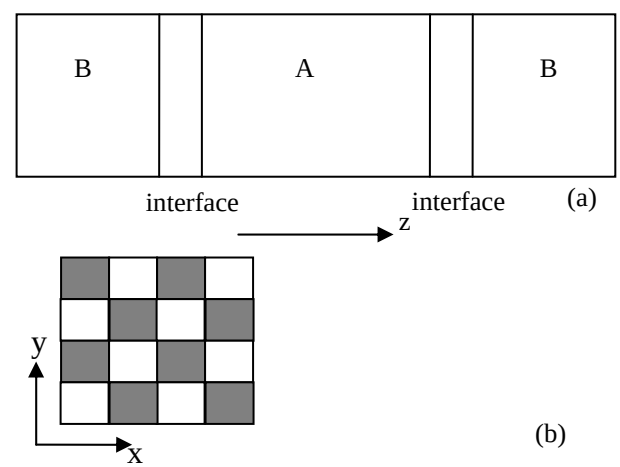

Figure 1(a) Simulation domain with two materials A and B, and a rough interface inserted in between. (b) A typical roughness structure at the interface, shown in cross-section. The white and gray squares refer to materials A and B, respectively. Each square is of width d.

PHONON WAVE PACKET METHOD

MD simulation yields information in the real position and momentum space. However, in order to observe phonon behavior, it is most convenient to analyze the data in phonon or wave-vector space. This requires a technique to transfer MD results, obtained in physical space and time, to phonon space so that phonon properties may be obtained. These post-processing techniques are described below.

The wave-packet technique is used in conjunction with MD simulation to investigate phonon transmission at interfaces. Treating phonons as a particle system, a wave packet with well-defined frequency and polarization may be defined. It is then possible to observe how this phonon (wave packet) propagates through the system. Schelling et al. [24] investigated how such a wave packet interacts with a coherent semiconductor interface using MD simulations. The transmission coefficients are obtained as a function of frequency for both longitudinal and transverse acoustic phonons.

The phonon wave packet is formed by a linear combination of system vibration eigenstates which can be obtained by diagonalizing the dynamical matrix of a perfect bulk crystal.

$$u_{in\mu} = A\varepsilon_{i\mu\lambda}(k_0)\exp[ik_0(z_n - z_0)]\exp[-(z_n - z_0)^2/\xi^2] \quad (1)$$

where $u_{in\mu}$ is the μth component of the displacement for atom *i* in the unit cell labeled by *n*. The phonon branch is labeled by λ and the wave amplitude is A; k_0 is wave vector and ε is the polarization vector and is calculated from lattice dynamics; z_n is the z coordinate of the unit cell n; the factor ξ is used to define the spatial width of the wave packet. Using this equation, a Gaussian wave packet is generated centered in real space around z_0 and in phonon space around k_0. The shape of the wave packet can be seen in real space, including the center and width. In order to observe how the wave packet spans k space, an inverse transformation must be performed. Since the wave packet is a linear combination of a series of wave functions, the contribution of different k values can be obtained by:

$$\psi(k) = \sum_i (\bar{\varepsilon}^*(k)\cdot\bar{u}_i)\exp[-ik(z_i - z_0)] \quad (2)$$

In order to generate the initial velocity of atoms, time-dependence is added to the normal modes using

$$u_{in\mu} = A\varepsilon_{i\mu\lambda}(k_0)\exp\{i[k_0(z_n - z_0) - \omega t]\}\exp[-(z_n - z_0)^2/\xi^2] \quad (3)$$

Differentiating this equation with respect to time yields the initial velocity.

This set of initial conditions perturbs the lattice from its equilibrium state, similar to pulling a string away from its equilibrium position. Once released, the generated wave is allowed to propagate. As the wave packet encounter the interface, part of it is reflected and the rest is transmitted. The proportion of energy being transmitted through the interface can be obtained by calculating the energy change in one of the sub-regions before and after the interface interaction. By repeating this process for all possible phonons, the transmission coefficient dependence on frequency and polarization can be determined. One may also investigate the conversion of phonon modes across the interface using Fourier transforms.

It should be pointed out that a large domain is generally required to localize the generated wave. The wave itself must have a sufficient spatial width to make sure that the spread in phonon space is tight enough. In addition, to treat phonons as particles, the wave packet size should be larger than the wavelength of the phonon of interest. Furthermore, for wave packets to have distinct interactions with each other, the distance they travel between collisions must be much greater than the size of wave packet. All these criteria lead to a very large length scale for the system. Typically, the wave packet size is 100-200 unit cells, and the entire domain length is 1000 unit cells. A limitation of this method is that it only treats modes in isolation. It has the possibility to handle multiple phonon modes with an assumption that they are linearly superposed. Hence, this simulation tool does not cover the real situation of many interacting modes incident on the interface simultaneously and coupled each other non-linearly.

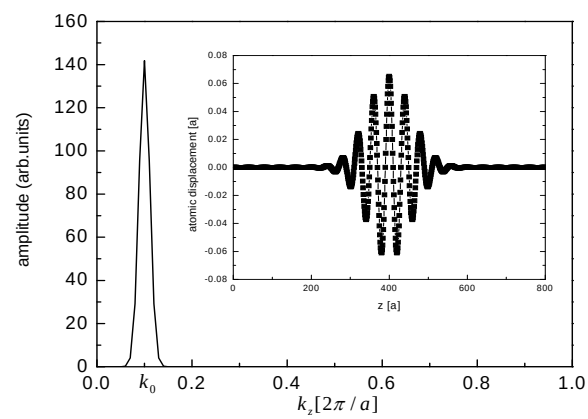

Figure 2. Illustration of a wave packet centered at $k_0 = 0.1[2\pi/a]$ and $z_0 = 400a$.

RESULTS

In this section, the wave packet method is applied to the investigation of phonon dynamics at different interfaces. The first step is to create a wave packet according to Eq.(1), corresponding to a specific phonon branch with a narrow frequency range and well-defined polarization. This wave packet is spatially centered at z_0 in real space and at k_0 in k space. The widths in physical and k space have an inverse relation. Therefore, in order to narrow down the extension in k space, the wave packet must span a wide region in real space. Figure 2 shows such a resulting wave packet centered at $k_0 = 0.1[2\pi/a]$ and $z_0 = 400a$ where a is the lattice constant. The contribution of different k values is shown, and the inset is the atomic displacement. Once the wave packet is created, it is allowed to propagate in both the z and (-z) directions through the simulation domain. Interface and boundary scattering and anharmonic effects will scatter the wave packet and damp propagation.

Smooth Interface

The first case to be considered is a perfectly smooth interface between materials A and B. A phonon wave packet is initialized at the center of material A, and then allowed to propagate towards material B. The lattice structure is constructed in such a way that the x, y, z axes correspond to the [100], [010] and [001] crystal directions respectively. The simulation domain has a dimension of 3x3x1000 cells, resulting in a length of 543 nm in z direction perpendicular to the interface and 1.6 side long in cross section. The simulation results are not sensitive to the size of cross-section area as long as the amplitude of the wave packet is small in comparison.

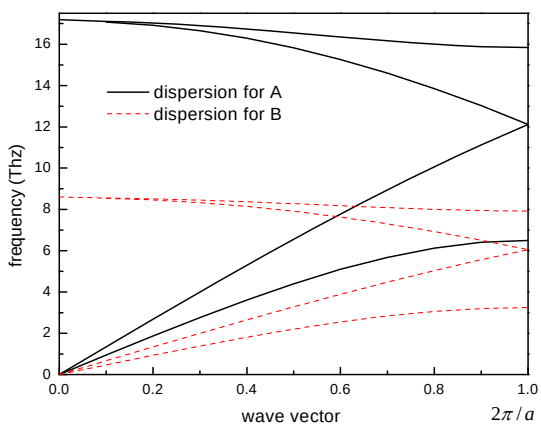

Figure 3. Dispersion relation for materials A and B in the [001] direction.

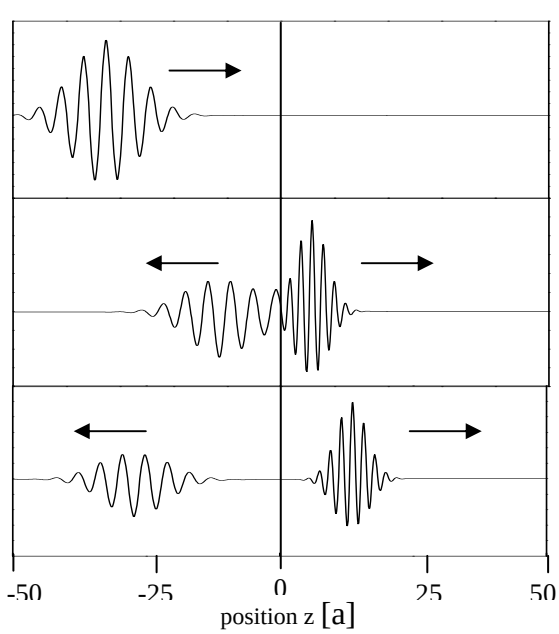

Figure 4. Snapshots of displacement (respectively at 0.1ps, 5ps and 7ps) for an LA wave packet with frequency 1.34 THz. Axis y is the vibration amplitude in arbitrary unit.

Because A and B only differ in atomic mass, they have the identical dispersion relation, expect that the frequency in B is only half of that in A, as shown in Fig. 3. Therefore, a cutoff frequency exists for phonon mode conversion. For instance, the highest frequency for the longitudinal-acoustic (LA) mode in material A (Si) is $f_A = 12.1THz$, while that in material B is $f_B = 6.1THz$. So, the maximum frequency for LA-LA conversion with non-zero transmission is 6.1 THz. Likewise, the highest frequency for the longitudinal-optical (LO) mode of material A is 17.2 THz; thus 8.6 THz is the cutoff frequency for LO-LO mode conversion.

Figure 4 shows a series of snapshots of a wave packet with $k_0 = 0.1[2\pi/a]$ and $f=1.34THz$ propagating through interface. After encountering the interface, part of the wave is transmitted and the rest is reflected. From this figure, the group velocity of incident, transmitted and reflected phonons can be calculated. Figure 5 illustrates the reflected and transmitted phonon distribution in k space assuming they are both LA branches. As shown in Fig. 5, the center of the reflected phonon packet is at $k_r = 0.1[2\pi/a]$. Thus the phonon frequency does not change before and after reflection. This indicates the reflected phonon has exactly the same character as the incident one. The transmitted phonon has a peak at $k_t = 0.22(2\pi/a)$. Referring to the dispersion of material B (Fig. 3), the corresponding frequency is found to be the same as that of the incident phonon. But the group velocity of transmitted phonons is reduced roughly by half compared to that of the reflected phonons. This is reasonable because the phonon wave propagates more slowly in material B since it is composed of heavier atoms.

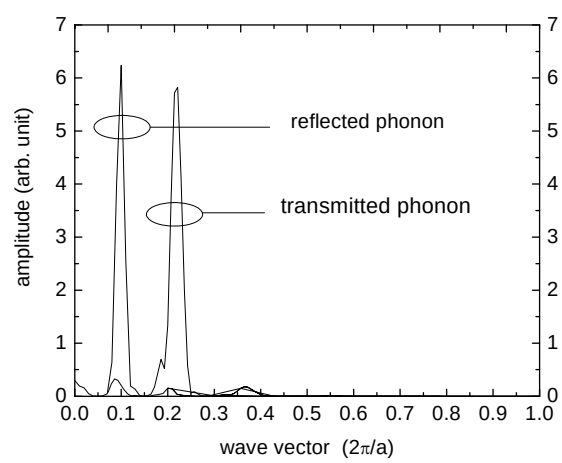

Figure 5. Distribution of reflected and transmitted phonons in k space.

The total energy in material A and B can be calculated by adding the potential and kinetic energies on each side. Figure 6 shows how the total energy changes with time as the wave packet propagates. The incident wave energy is normalized as one. Here we define the transmission coefficient as the ratio of the energy transmitted to side B and the initial energy on side A. By quantifying the energy change, transmission

coefficients can be obtained. The frequency-dependence of the energy transmission coefficient for incident LA wave packets is shown in Fig. 7. At the low frequency limit, the acoustic match (AM) assumption is valid and the transmission coefficient for phonon transport between materials A and B may be found to be:

$$t_{AB} = \frac{4Z_A Z_B}{(Z_A + Z_B)^2} \tag{4}$$

where $Z = \rho c$ is acoustic impedance, ρ is mass density and c is speed of sound respectively. This formula gives a transmission coefficient value of 0.89 based on the mass difference This estimation matches well with the MD prediction. As the frequency increases, a smoothly decreasing trend is seen. A nearly zero transmission beyond the cutoff frequency of 8.6 THz is observed, as expected.

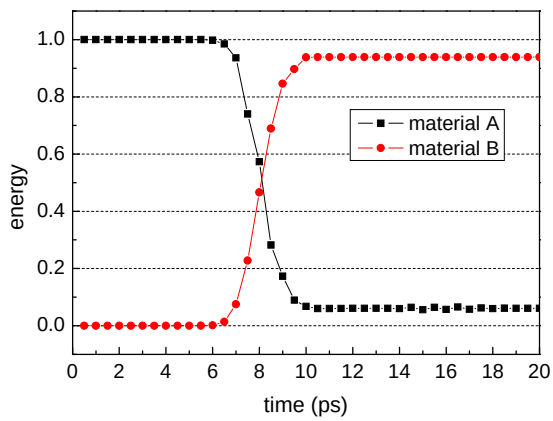

Figure 6. Energy change with time for material A and B.

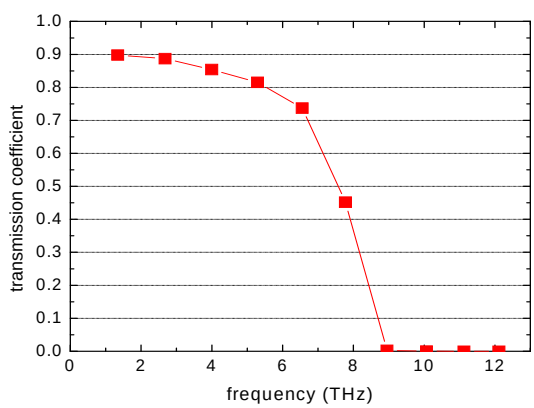

Figure 7. Energy transmission coefficient for LA wave packets.

Since the incident phonon frequency is smaller than 6.1THz, both the transmitted and reflected phonons fall on the longitudinal acoustic branch. In this regime, phonons encounter elastic scattering at the interface and their frequency does not change. When the frequency is between 6.1THz and 8.6 THz, the transmitted phonon is optical. Inelastic scattering must happen at the interface to modify the phonon mode from acoustic to optical. When the frequency is beyond 8.6 THz, there is only a very small fraction of phonons that can be transmitted. The transmitted phonons have very long wavelengths and carry a very small amount of energy.

Interface with Random Roughness

Next a layer of random roughness is inserted between materials A and B. In order to isolate the effect of random roughness without the complication of mass differences, the baseline system consists entirely of material A; a transmission coefficient of unity would be obtained in the absence of the rough interface. A layer of roughness of specified width is created at the center of the domain. The random roughness is created by mixing a group of atoms with different masses. The atomic mass of each random atom is defined centered on the properties of material A by using a series of random numbers.

Table1: LA phonon transmission coefficient at an interface with random roughness.

Case 1: Mass range 0.9~1.1; roughness thickness 5a.					
k	0.1	0.3	0.5	0.7	0.9
T	0.99	0.97	0.95	0.93	0.91
Case 2: Mass range 0.5~1.5; roughness thickness 5a.					
k	0.1	0.3	0.5	0.7	0.9
T	0.99	0.83	0.65	0.53	0.36
Case 3: Mass range 0.5~1.5; roughness thickness 10a					
k	0.1	0.3	0.5	0.7	0.9
T	0.99	0.76	0.51	0.39	0.22

Table 1 shows the phonon transmission coefficient for three cases assuming the incident phonons are all LA branches. k refers to wave vector and T means transmission coefficient. In Case 1, the interface thickness is 5 a, (a is lattice constant) and the assigned random atomic masses range from 0.9 to 1.1 of material A. In Case 2, the interface thickness keeps the same as Case 1 but the mass range is increased, causing a larger jump in properties at the interface. In Case 3, the interface thickness is increased while keeping the mass range the same as in Case 2. It may be seen from Table 1 that the randomly rough interface located inside a homogeneous material becomes the scattering source for incident phonons and interact with them. The phonons with long wavelength have a higher transmission coefficient than the short ones. The thicker the interface is, the more scattering events occur and thus the smaller the transmission is. Furthermore, the mass variance at the interface is another important factor in decreasing the transmission coefficient; significant decreases occur for all but the longest wavelengths.

Interface with Structured Roughness

Still using the homogeneous system as a baseline, a superlattice structure is inserted at the interface instead of random roughness. The superlattice is created by repeating the A and B materials in layers. Different combinations of layer thickness and number of layers are investigated for the transmission of LA phonons, and some typical cases are shown in Table 2. Here, the thickness is that of each periodic layer in the superlattice structure, N is the number of repeating layers, and k is wave number of the incident phonon. A great difference compared to random roughness cases is that when

the thickness of the interface gets larger, the phonon transmission is not found to decrease significantly. This is due to the periodic structure at interface. When phonon waves propagate through the superlattice layers, strong wave interference takes place because of the structural periodicity and the superimposition of different modes may generate new channels for phonon transmission. These new phonon paths restore the transmission reduction caused by scattering; this effect has also been noted by Simkin and Mahan [25]. As before, the longer wavelength phonons generally exhibit higher transmission coefficients. Furthermore, an asymptotic transmission coefficient value is reached as the number of layers increases beyond N=8 or so.

Table 2. Phonon transmission coefficient at superlattice-structured interface for LA phonons

Case1: k=0.1 thickness=2a			
N=2	N=4	N=10	N=20
0.91	0.90	0.92	0.91
Case2: k=0.1 thickness =10a			
N=2	N=4	N=8	N=20
0.80	0.75	0.69	0.65
Case3: k=0.5 thickness=2a			
N=2	N=4	N=8	N=20
0.65	0.59	0.54	0.52
Case4: k=0.5 thickness=5a			
N=2	N=4	N=8	N=20
0.59	0.53	0.43	0.41

Structured Interfaces Between Heterogeneous Materials

We now examine structured rough interfaces in heterogeneous systems. In the simulation domain shown in Fig. 1a, a layer of roughness is inserted by staggering materials A and B cell by cell (see Fig. 1b). Material A and B both have a length of 1000 unit cells. At the initial moment, the wave packe is located at the center of domain. After released, the wave propagates along both directions and encounters the A/B interface after a while. Since the system is fully symmetric along the center of the domain, we only focus on one of the interfaces. The reason that the system is set in such a way is to accommodate the periodic boundaries condition easily. The dependence of the transmission coefficient for LA phonons on rough layer thickness was tested holding the width d of each A/B periodic unit to one unit cell thickness, a.

Table 3: Phonon transmission at structured heterogeneous interface for LA phonons

Group 1. k=0.05						
Thickness [a]	0	1	2	4	10	50
Transmission	0.91	0.92	0.90	0.90	0.89	0.89
Group 2. k=0.5						
Thickness [a]	0	1	2	4	10	50
Transmission	0.73	0.32	0.15	0.245	0.27	0.44
Group 3. k=0.7						
Thickness [a]	0	1	2	4	10	50
Transmission	0.05	0.04	0.05	0.03	0.06	0.04

Table 3 shows the phonon transmission coefficient as a function of thickness for three typical phonon groups: long wavelength, medium wavelength and short wavelength. The rough layer thickness ranges from 0 to 50 unit cells. Zero thickness corresponds to the smooth interface case discussed earlier. Group 1 refers to those phonons that have the low frequency and long wavelength. In this range, phonons behave like harmonic plane waves and the typical wavelength is far greater than the roughness thickness. When the wave encounters the roughness, the phonon wave simply passes over the roughness and has almost no interaction with the interface. Therefore, the transmission coefficient is nearly unity, similar to that of the ideal interface.

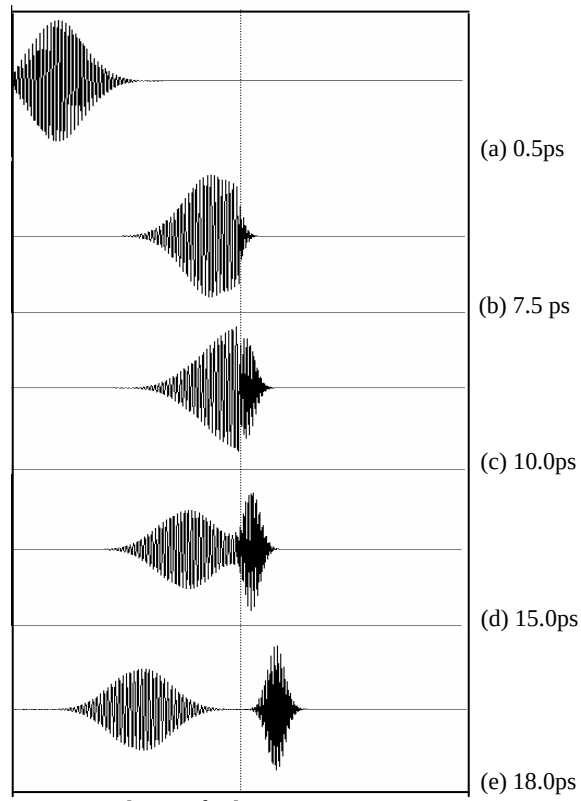

Figure 8. Snapshots of phonon propagation at a structured rough heterogeneous interface interface with k=0.5. Y axis shows the displacement amplitude.

For Group 2, the wave number value is approximately midway between the center and edge of the Brillouin zone. The phonon transmissivity is seen to change significantly with rough layer thickness. When the roughness thickness is comparable to wave length, which is at the order of 2nm, the phonon transmission is greatly reduced by 30%-50%. Figure 8 shows the snapshots of phonon propagation when k=0.5.

Figure 9 shows the energy change with time for materials A and B and the interface region. The incoming phonon waves encounter the front interface at 7.5ps. Some phonons are then reflected back into material A and others go into the interface layer. These phonons bounce back and forth inside the rough layer for a short time. Gradually, they either transmitted back to A or to B and the total energy is conserved.

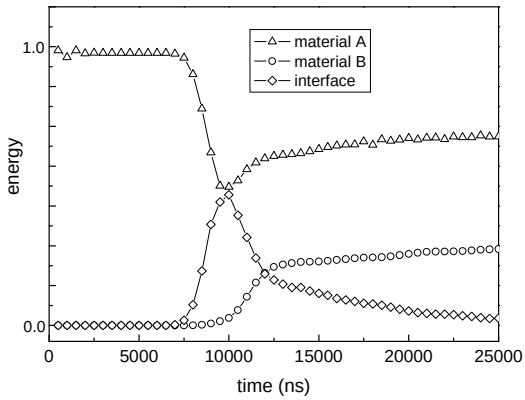

Figure 9: Energy change with time for material A and B and interface for phonon transport across a structured heterogeneous interface for k=0.5 and a roughness layer thickness of 4a. Incident energy is unitized as one.

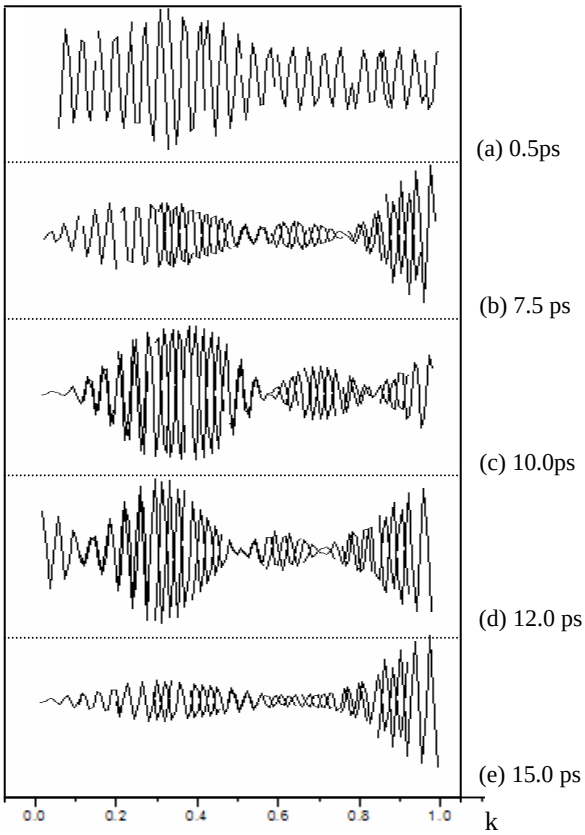

Figure 10. Phonon distribution in k space evolution with time in interface region. Axis y shows the amplitude in arbitrary unit.

By analyzing the data in phonon space, complex and strong phonon interactions are observed while phonons vibrate inside the interface. Figure 10 shows the evolution of phonon distribution inside the rough interface region. In the beginning, when incoming phonon wave is still far away, the phonons inside the interface are randomly distributed and the energy is at a very low level. When phonons begin to contact interface, (see Fig. 8b and 10b at 7.5ps), phonon spectrum spans widely and contains a number of frequencies not contained in the original incident wave. This indicates that multiple phonon modes are generated due to the contact. Furthermore, these newly developed modes interact with one another and assemble or disperse to other modes (Fig. 10b-d). At the end of interface interaction, all the phonons are finally converted two groups, one is in low frequency range and the other is at the edge of Brillouin zone (Fig. 10e).

After all the phonons leave the interface, the phonons of material A are concentrated at k=0.5, the same as the incident phonons. The phonons of material B are concentrated at k=1.0, corresponding to the incident frequency of 6.1 THz for the dispersion curve of material B. This is shown in Fig. 11. Although it is difficult to quantify the connection between these complex phonon dynamics and the trends in the transmission coefficient with layer thickness, these phonon conversions at the interface could be one reason for the great reduction in phonon transmission coefficient for Group 2 in Table 3. Furthermore, the transmission coefficient exhibits a minimum at a layer thickness of 2a but recovers to a higher value of 0.44 for a layer thickness of 50a. One reason for this could be the presence of a regular periodic structure, similar to superlattices. As discussed in the previous section, wave interference effects due to periodicity would act to restore the phonon transmission past its minimum.

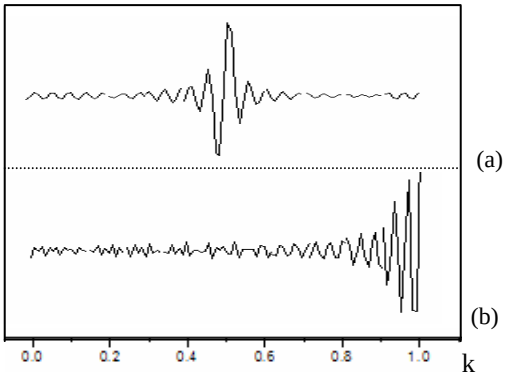

Figure 11. Distribution in k space for reflected phonon in material A (a) and transmitted phonon in material B (b) after interface interaction at 20ps.

For Group 3, the associated phonon wavelengths are close to the cutoff frequency, where the transmission is expected to be zero. The phonon scattering mechanism may be changed due to the interface roughness but does not cause a significant change in the phonon transmission. Moreover, at the room temperature, the phonon occupation number in this frequency range is relatively small, making the transmission coefficient in this range not crucial for most practical applications.

The final case explores the effect of the in-plane roughness structure on the transport of LA phonons. The interface thickness is fixed at 2a. On a cross-sectional area of 20x20 cells, a structured roughness pattern is created, as shown in Fig. 1b. The width d of each square in Fig. 1b is varied from 1

to 10a. The simulation results, summarized in Table 4, show that the phonon transmission coefficient does not change significantly with in-plane atomic structure. This is because the incoming phonons are longitudinal acoustic phonons and vibrate only along the z direction. Some transverse modes may be activated at the interface, but not in large-enough amounts to matter. The thickness of the rough layer in the z direction is the dominant factor since it is aligned with the phonon propagation direction; in contrast, the transmission coefficient is insensitive to the structure in the x-y plane. In order to confirm this statement, further work must be performed to study the transport of transverse acoustic phonons at interfaces. For these, the roughness structure in x-y plane is expected to influence transmission to a greater extent.

Table 4. Phonon transmission coefficient variation with change in in-plane roughness structure for LA phonons

d [a]	<1	1	2	4	8	10
Transmission	0.33	0.40	0.42	0.447	0.475	0.41

CONCLUSIONS

Detailed phonon scattering at a rough semiconductor interface is studied by molecular dynamics simulations. Two diamond-structured materials that differ only in their masses are chosen. The interface between these two semiconductors is manipulated to create a thin layer of roughness by staggering the two types of atoms at the interface. The roughness is characterized by the interval space between these two different types of atoms on the interface plane and also the thickness of the interface layer. A phonon wave packet is initialized with a pre-defined frequency and polarization and allowed to propagate through the interface. The interaction of phonon wave packet with the interface is monitored by analyzing the resulting displacement-versus-time signal in phonon wave space. The phonon transmission coefficient is calculated by measuring the phonon energy change before and after the interface scattering.

For an ideal (smooth) interface, the transmission coefficients predicted by the MD simulations agree well with the acoustic mismatch model based on the continuum assumption. The rough interface simulation results indicate that random roughness is the source of phonon scattering and decreases the phonon transmission.

Periodic structure causes strong phonon wave interference and may restore phonon transmission. For these structures, the phonon transmission coefficient is a strong function of frequency and the roughness characteristic length. In the low-frequency limit, the roughness structure at interfaces is transparent to acoustic phonons and the transmission coefficients equal the ideal-interface results. In the mid-frequency range, phonon transmission is significantly decreased when the roughness characteristic length is comparable to the phonon wave length. Complex phonon mode conversions are observed and wave interference at this range is conjectured to be the reason for decreased transmission. At frequencies close to the cutoff frequency, the transmission coefficients drop rapidly to zero and the roughness influence is not evident.

ACKNOWLEDGEMENTS

Support under NSF grants CTS-0312420, CTS-0219098, and DARPA's IMPACT Center, and the computational resources of Purdue's Network for Computational Nanotechnology (NCN) are gratefully acknowledged.

REFERENCES

[1] M. Asheghi, M.N. Touzelbaev, et al, "Temperature-Dependent Thermal Conductivity of Single-Crystal Silicon Layers in SOI Substrates," ASME Journal of Heat Transfer, Vol. 120, pp. 31-36. 1998.

[2] E. S. Snow, J. P. Novak, et al, "Random networks of carbon nanotubes as an electronic material," Appl. Phys. Lett., 82(13), pp. 2145-2147, 2003.

[3] X. Duan, C. Niu, et al, "High-performance thin-film transistors using semiconductor nanowires and nanoribbons," Nature, 425, pp. 274-278, 2003.

[4] J. Xu and T. S. Fisher, "Enhancement of thermal interface materials with carbon nanotube arrays", International Journal of Heat and Mass Transfer, 49, pp. 1658-1666, 2006.

[5] P.L. Kapitza, "the Study of Heat Transfer in Helium II", Zhurnal eksperimental noi i teoreticheskoi fiziki, Vol. 11, pp1-31, 1941.

[6] I.M. Khalatnikov and I.N. Adamenko, "Theory of the Kapitza Temperature Discontinuity at a solid body-liquid helium boundary", Sovied Physics JETP, Vol. 36, pp391, 1973.

[7] E.T. Swartz and R.O. Pohl, "Thermal resistance at interfaces", Applied Physics Letters, Vol. 51, pp2200, 1987.

[8] R. J. Stevens, P. M. Norris, et al, "Molecular-Dynamics Study of Thermal Boundary Resistance: Evidence of Strong Inelastic Scattering Transport Channels", Proceedings of IMECE, Anaheim, CA, 2004.

[9] G. Burkhard, A.B. Sawaoka, et al, "The effect of Umklapp processes on the heat transport of solids", Proc., The Symposium on Thermal Science and Engineering in Honor of Chancellor Chang-Lin Tien, eds., University of California Berkeley, California, pp145-152, 1995.

[10] R.J. Stoner and H.J. Maris, "Kapitza conductance and heat flow between solids at temperatures from 50 to 300K", Physical Review B, Vol. 48, pp16373, 1993.

[11] D.A. Young and H.J. Maris, "Lattice-Dynamical Calculation of the Kapitza Resistance between FCC Lattices", Physical Review B, Vol. 40, pp3685, 1989.

[12] H. Zhao and J. B. Freund, "Lattice-dynamical calculation of phonon scattering at ideal Si-Ge interfaces", Journal of Applied Physics, Vol. 97, pp024903, 2005.

[13] N. Mingo and L. Yang, "Phonon transport in nanowires coated with an amorphous material: An atomistic Green's function approach", Physical Review B 68, 245406, 2003.

[14] W. Zhang, N.Mingo et al, , "Simulation of Interfacial Phonon Transport in Si-Ge Heterostructures using an Atomistic Green's Function Method", Journal of Heat Transfer, Vol 129, pp. 483-491, 2007.

[15] S.-H. Choi and S. Maruyama, "Thermal Boundary Resistance at an Epitaxially Perfect Interface of Thin Films", International Journal of Thermal Sciences, Vol. 44, pp547-558, 2005.

[16] Phil J. Hegedusa and Alexis R. Abramson, "A molecular dynamics study of interfacial thermal transport in

heterogeneous systems", International Journal of Heat and Mass Transfer, Vol. 49, pp4921-4931, 2006.
[17] Xin-Gang Liang, B. Yue, et al., "Simulation of Interface Structure Influence on in-Plane Thermal Conductivity of Ar-Like Nano Films by Molecular Dynamics", Journal of Enhanced Heat Transfer, Vol. 14, pp233-242, 2007.
[18] A. Maiti, G.D. Mahan, et al, "Dynamical Simulation of Nonequilibrium Processes- Heat Flow and the Kapitza Resistance Across Grain Boundaries", Solid State Communications, Vol 102, pp517, 1997.
[19] P. K. Schelling, S. R. Phillpot, et al, "Kapitza Conductance and phonon Scattering at Grain Boundaries by Simulation", Journal of Applied Physics. Vol. 95, pp6082, 2005.
[20] P. K. Schelling, S. R.Phillpot, et al, "Phonon Wave-Packet Dynamics at Semiconductor Interfaces by Molecular_Dynamics Simulation", Applied Physics Letters, Vol. 80, pp2484, 2002.
[21] C.J. Twu and J.R. Ho, "Molecular dynamics study of energy flow and the Kaptiza conductance across an interface with iimperfection formed by two dielectric thin films", Physical Review B, 67, pp205422, 2003.
[22] M. Z. Bazant, E. Kaxiras, et al, "Environment Dependent Interatomic Potential for Bulk Silicon", Phys. Rev. B 56, pp8542, 1997.
[23] L. Sun, C. Le, et al, "Performance of a parallel molecular dynamics program for computation of thermal properties", Numerical Heat Transfer, 51, pp. 315-331, 2007.
[24] P.K. Schelling, S.R.Phillpot, et al, "Phonon wave-packet dynamics at semiconductor interfaces by molecular dynamics simulation", Applied Physics Letters, Vol. 80, 2484-2486, 2002.
[25] M.V. Simkin and G. D. Mahan, "Minimum Thermal Conductivity of Superlattices", Physical Review letters, Vol 84, pp927, 2000.